CARBON 47 (2009) 493–499

available at www.sciencedirect.com

ScienceDirect

journal homepage: www.elsevier.com/locate/carbon

Synthesis of high-quality graphene with a pre-determined number of layers

Zhong-Shuai Wu, Wencai Ren, Libo Gao, Bilu Liu, Chuanbin Jiang, Hui-Ming Cheng**

Shenyang National Laboratory for Materials Science, Institute of Metal Research, Chinese Academy of Sciences, 72 Wenhua Road, Shenyang 110016, PR China

ARTICLE INFO

Article history:
Received 27 June 2008
Accepted 20 October 2008
Available online 5 November 2008

ABSTRACT

A simple and effective strategy is proposed to tune the number of graphene layers by selecting suitable starting graphite, using a chemical exfoliation method. It is found that both the lateral size and the crystallinity of the starting graphite play important roles in the number of graphene layers obtained. Using artificial graphite, flake graphite powder, Kish graphite, and natural flake graphite as starting materials, ~80% of the final products are single-layer, single- and double-layer, double- and triple-layer, and few-layer (4–10 layers) graphene, respectively, while a mixture of few-layer (4–10 layers) and thick graphene (>10 layers) is obtained when highly-oriented pyrolytic graphite is used. The smaller the lateral size and the lower the crystallinity of the starting graphite, the fewer the number of graphene layers obtained. Moreover, the graphenes obtained are of high-quality with an electrical conductivity of $\sim 1 \times 10^3$ S/cm. These findings open up the possibility for controlled production of high-quality graphene with a selected number of layers in a large quantity.

1. Introduction

Graphene shows great importance for fundamental studies and technological applications due to its unique structure and a wide range of unusual properties [1]. Its electron transport is described by the relativistic-like Dirac equation, and this allows access to the rich and subtle physics of quantum electrodynamics in relatively simple condensed matter experiments [2–5]. The scalability of graphene devices to true nanometer dimensions makes it a promising candidate for future electronics because of its ballistic transport at room temperature combined with chemical and mechanical stability [6]. In addition, graphene also exhibits great promise for potential applications in many other technological fields [1,7–12] such as sensors, composites, supercapacitors, transparent conductive films, solar cell and gas storage media. However, the properties of graphene strongly depend on their structures. For example, a variation of the number of graphene layers may result in a striking change of their electronic properties [1]. Accordingly, it is very important to explore the production of graphene with a selected number of layers in large quantities for their further fundamental studies and extensive applications.

Currently, several methods have been proposed to prepare graphene, such as micro-mechanical cleavage [2], epitaxial growth on SiC wafer [13] and chemical exfoliation [14–20]. For the first two methods, both the productivity and layer selectivity of graphene are poor. A chemical exfoliation strategy from bulk graphite has been suggested to be an effective general way to produce graphene in a large quantity and at low cost [15,16], in which a process of graphite oxidation and/or thermal expansion of graphite oxide (GO)/expandable graphite is involved. During oxidation, the introduction of oxygen-containing functional groups such as hydroxyl and

* *Corresponding authors:* Fax: +86 24 2390 3126.
E-mail addresses: wcren@imr.ac.cn (W.C. Ren), cheng@imr.ac.cn (H.-M. Cheng).
0008-6223/$ - see front matter
doi:10.1016/j.carbon.2008.10.031

epoxide reduces interlayer interactions and results in an increase in the *d*-spacing of GO, thereby promoting complete exfoliation of single GO layers in some specific conditions. By using the chemical exfoliation method, single-layer graphene has been prepared. For example, Ruoff and co-workers prepared single-layer graphene by exfoliation of GO via ultrasonic treatment, followed by chemical reduction with hydrazine hydrate to modify their transport properties [15]. Schniepp et al. prepared functionalized graphene by oxidation of graphite and subsequent thermal expansion/exfoliation of GO with rapid heating [16]. Very recently, Li et al. fabricated ultra-smooth graphene nanoribbons by combining thermal exfoliation of expandable graphite with chemomechanical breaking of the resulting graphene sheets by sonication [19]. However, the selective production of high-quality graphene with a selected number of layers in a large quantity still remains a significant challenge.

We have studied the effect of the lateral size and crystallinity of starting graphite materials on the number of graphene layers by the chemical exfoliation method. It is interesting to find that both the lateral size and the crystallinity of the starting graphite materials play important roles in the number of graphene layers produced, and the majority of graphene can be tuned to a specific number of layers by selecting suitable starting graphite. For example, artificial graphite, a graphite with a small lateral size and low crystallinity, is suitable for the production of single-layer graphene. Also, we found that this graphene has high electrical conductivity.

2. Experimental

2.1. Materials

Five types of graphite materials: highly-oriented pyrolytic graphite (HOPG), natural flake graphite (NFG, Qingdao Black Dragon Graphite Co., Ltd), Kish graphite (KG, Sinopharm Chemical Reagent Co., Ltd), flake graphite powder (FGP, Sinopharm Chemical Reagent Co., Ltd) and artificial graphite (AG, Qingdao Black Dragon Graphite Co., Ltd), were used as the starting materials to demonstrate the production of graphene with a selected number of layers using chemical exfoliation.

2.2. Preparation of graphene

The preparation of graphene involves three key steps, (i) oxidation of the starting graphite to synthesize GO, (ii) thermal expansion/exfoliation of the as-prepared GO to obtain thermally expanded GO (TEGO), and (iii) reduction and dispersion of the resulting TEGO to produce graphene. It should be emphasized that, for comparison, all the experimental procedures related to the synthesis of GO, TEGO and graphene from the five starting graphites were performed under the same conditions.

2.2.1. Synthesis of GO

We used the Hummer method [21] to oxidize the different starting graphites for the synthesis of GO. First, 2 g graphite, 1 g sodium nitrate and 46 mL of sulfuric acid were mixed and strongly stirred at 0 °C for 15 min in a 500 mL reaction flask immersed in a water-glycol bath (DFY-5 L/25). Then 6 g potassium permanganate was added slowly to the above solution and cooled for 15 min. After this, the suspended solution was stirred continuously for 1 h, and 92 mL of water was added slowly to the suspension for 10 min. Subsequently, the suspension was diluted by 280 mL of warm water and treated with 10 mL of H_2O_2 (30%) to reduce residual permanganate to soluble manganese ions. Finally, the resulting suspension was filtered, washed with water, and dried in a vacuum oven at 60 °C for 24 h to obtain GO.

2.2.2. Thermal expansion/exfoliation of GO

The as-prepared GO was thermally expanded to synthesize TEGO by rapidly heating it in a Lindberg tube furnace. Generally, the as-prepared GO was first loaded in a quartz boat of length 100 mm and diameter 20 mm, which was then inserted into a 1.5 m-long quartz tube with inner diameter of 22 mm and outer diameter of 25 mm. After the tube furnace was heated to 1050 °C and argon was flowed though the tube for 10 min, with a flow rate of 200 mL/min, the sample boat of GO placed in the quartz tube was rapidly moved into the middle heating zone of the furnace and kept there for 30 s, before being quickly removed from the heating zone.

2.2.3. Reduction and dispersion of TEGO

The resulting TEGO was first reduced by H_2 for 2 h at 450 °C in a gas flow of H_2 (100 mL/min) and argon (100 mL/min). Then, the reduced TEGO platelets were stirred for 1 h in a solution of *N*-methylpyrolidone (NMP) before being dispersed for 2 h at 40 °C by sonication to form a homogenous suspension. Finally, centrifugation was used to remove thick multilayer pieces and not fully exfoliated graphite flakes from the TEGO-generation process, and to retain the thin graphene sheets in the supernatant.

2.3. Material characterization

X-ray photoelectron spectroscopy (XPS, Escalab 250, Al kα), atomic force microscopy (AFM, Veeco MultiMode/NanoScope IIIa), scanning electron microscopy (SEM, LEO, Supra 35, 15 kV), high-resolution transmission electron microscopy (HRTEM, JEOL JEM-2010, 200 kV, and Technai F30, 300 kV), and nitrogen cryosorption (Micromeritics, ASAP2010M) were used to characterize the GO, TEGO and graphene. It is necessary to point out that the supernatant was dropped onto grids with a holey carbon film for SEM investigations.

2.4. Electrical conductivity measurement

The electrical conductivity of graphene was measured inside a JEOL JEM-2010 HRTEM equipped with a Nanofactory TEM-scanning tunneling microscopy (STM) system (ST1000), which integrates a fully functional STM into a HRTEM. The STM probe was controlled by a piezo-manipulator that can approach individual nanostructures inside the HRTEM. The obtained supernatant after centrifugation treatment was filtered and then dried in a vacuum oven at 60 °C for 24 h. The resulting graphene powders were attached to an Au electrode, and the tungsten STM tip was controlled precisely in

the HRTEM to connect to the graphene to measure its electronic conductivity.

3. Results and discussion

Fig. 1 shows the typical SEM images of the different starting graphites used in our experiment. HOPG, consisting of a highly ordered stack of graphene layers along the c-axis, has a large lateral size (referring to the particle size along the plane direction perpendicular to the c-axis) of more than 1000 μm. NFG has a plate-like morphology with a size of >600 μm and thickness of several micrometers, and FGP has a mean lateral size of <30 μm. Note that these two types of flake graphite are single crystal graphite with high purity. KG (>200 μm) was obtained by the crystallinization of carbon in molten steel during the manufacturing process. It has a high crystallinity but lower than HOPG and NFG. As to AG, it has an average lateral size of less than 30 μm, and lower crystallinity than HOPG and flake graphite but higher than KG.

AFM was used to examine the detailed structure of the synthesized samples after spin-coating the supernatant onto a 300 nm SiO_2/Si substrate. It was found that most of the graphene shows a relative smooth planar structure (Fig. 2a), similar to that obtained by mircomechanical cleavage [2]. This was further verified by SEM (Fig. 2b) and TEM (Fig. 2c) observations, indicating the high-quality of these graphenes. In addition, XPS measurements revealed that the C/O ratio (10.8–14.9) of the TEGO reduced by H_2 is evidently more than that of GO (1.7–2.5) and TEGO (5.6–7.9), and the corresponding C1s peak structure of the reduced TEGO is similar to that of pristine HOPG, without significant signals corresponding to the C–O species of GO (Fig. 3). These results suggest that the final graphene is reduced by the thermal expansion and reduction processes, without excessive covalent chemical functionalization as in the case of GO. It is worth noting that no significant holes were found in the platelets although most of the functional groups were removed during thermal expansion and H_2 reduction processes (Fig. 2c).

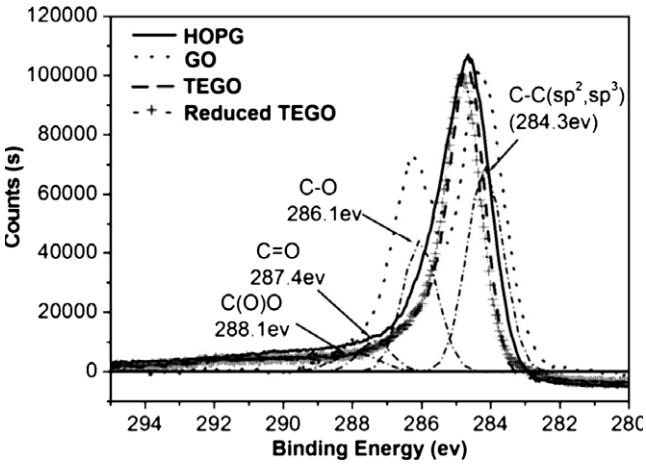

Fig. 3 – The C1s XPS spectra of GO, TEGO, reduced TEGO, and pristine HOPG. The C1s XPS spectrum of GO clearly indicates a considerable degree of oxidation with four components that correspond to non-oxygenated ring C (284.3 eV), C in C–O bonds (286.1 eV), carbonyl C (287.4 eV), and carboxylate carbon (O–C=O, 288.1 eV).

A great number of AFM measurements were performed to determine the number of graphene layers prepared from different starting graphite materials. Fig. 4a–c shows the typical AFM images of the graphene derived from KG, FGP, and AG, respectively. In order to determine the number of layers of the obtained graphenes according to the AFM measurements, it is prerequisite to know the thickness and interlayer spacing of the graphenes with different number of layers. It has been theoretically predicted that the interlayer spacing of GO is ~0.7 nm, due to a 0.44 nm increase in graphene thickness

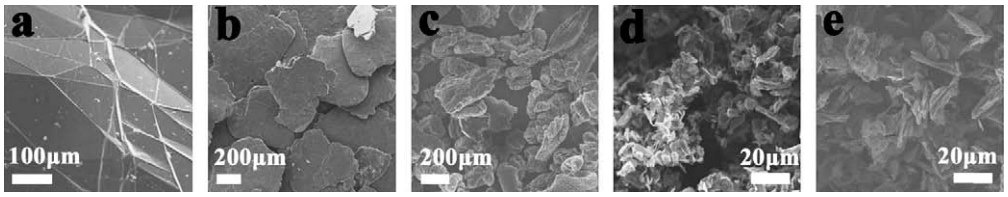

Fig. 1 – Typical SEM images of (a) HOPG, (b) NFG, (c) KG, (d) FGP, and (e) AG.

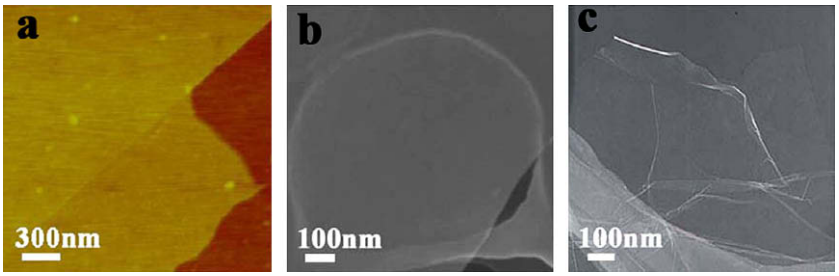

Fig. 2 – Typical morphology of the graphene derived from AG. (a) AFM image of the graphene on a SiO_2/Si wafer, displaying a relative smooth planar structure. (b) SEM image of the graphene hanging over a holey carbon film, showing a flat and transparent structure. (c) TEM image of the graphene.

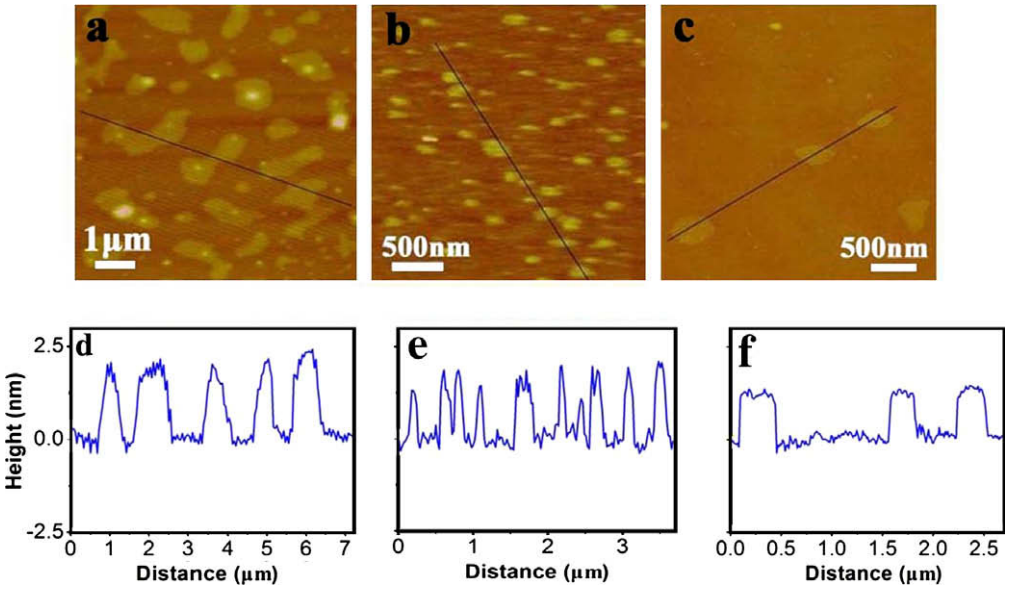

Fig. 4 – Tapping-mode AFM images and the corresponding height profiles of the graphenes derived from (a) and (d) KG, (b) and (e) FGP, and (c) and (f) AG. The thicknesses of the graphenes are 1.9–2.3 nm, 1.3–2.1 nm, and 1.1–1.3 nm, respectively, for KG, FGP, and AG as starting materials.

caused by the presence of epoxy and hydroxyl groups on both sides of the surface [16,17]. This result has also been experimentally proved by many groups based on AFM observations, and the thickness of a chemically derived single-layer graphene was found to be ~1.1 nm [15–17,22,23]. In order to obtain the structural information of our graphene, we performed a great deal of HRTEM observations. Fig. 5 shows the typical HRTEM images of the obtained graphenes with different number of layers. The folded structure of graphene edges allows for the evaluation about their thickness and interlayer spacing. It is worth noting that, different from graphite, the adjacent graphene layers of double- and triple-layer graphenes derived from chemical exfoliation are not parallel but uneven. The maximum thicknesses of single-, double-, and triple-layer graphenes derived from HRTEM images are ~0.57, 1.25, and 1.83 nm, respectively. Based on the above XPS analyses, we believe that there exist some residual functional groups on the surface of graphene although most of them have been removed during the thermal expansion and H_2 reduction processes, and these functional groups can not be directly probed by HRTEM. According to the measured thicknesses of single-, double-, and triple-layer graphenes, the interlayer spacing can be calculated to be in the range of ~0.55–0.70 nm. Obviously, this value is much larger than that of graphite, normally 0.335 nm. This spacing increase, ~0.21–0.36 nm, is consistent with that theoretically predicted for functional groups on the graphene surface [16,17]. As a consequence, the real thickness of the obtained graphene should be the sum of the observed thickness from HRTEM and the thickness increase caused by the presence of epoxy and hydroxyl groups on both sides of the surface. With 0.36 nm thickness increase, the real thickness of single-, double-, and triple-layer graphenes was evaluated to be ~0.93, 1.61 and 2.19 nm, respectively. Taking into account of the increased spacing or instrumental offset between the substrate and graphene sheet [16,17,24], in our calculations, we adopt 1.1 nm and 0.7 nm as the average thickness of single-layer graphene and the interlayer spacing, respectively. The topographic height distributions (Fig. 6a), derived from AFM measurements on 100 sheets for each starting material and based

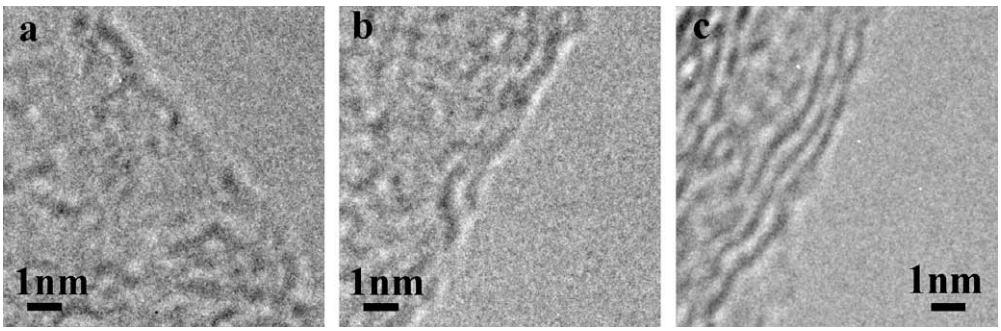

Fig. 5 – Typical HRTEM images of (a) single-, (b) double-, and (c) triple-layer graphene sheets with folded edges obtained by chemical exfoliation.

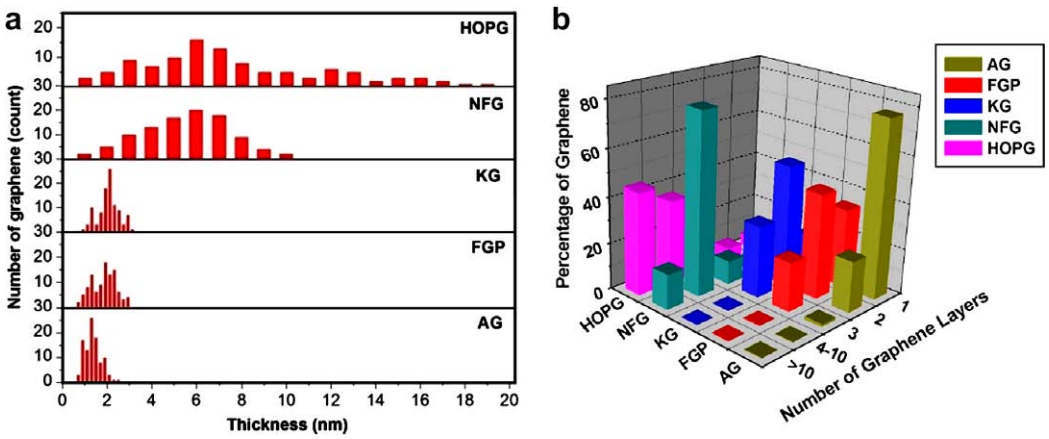

Fig. 6 – Statistical distributions of the thickness and the number of layers of the graphenes prepared from different starting graphites. (a) Histograms of the thickness distribution of graphene derived from HOPG, NFG, KG, FGP, and AG, obtained from 100 graphenes for each sample. (b) Histogram of the distribution of the number of graphene layers, obtained from the corresponding thickness distribution in (a).

on a Gaussian fit, indicate that the graphenes prepared from AG, FGP, KG, NFG and HOPG have a mean thickness of 1.30, 1.87, 2.05, 5.75 and 6.19 nm, respectively. Consequently, the layer-number distribution of our graphene can be obtained, as shown in Fig. 6b. It is interesting to find that ~80% of the final products are single-layer, single- and double-layer, double- and triple-layer, and few-layer (4–10 layers) graphene, respectively, from AG, FGP, KG, and NFG as starting materials, while a mixture of few-layer (4–10 layers) and thick graphene (>10 layers) is obtained when HOPG is used. These results suggest that the number of layers for chemically derived graphene can be tuned by selecting suitable starting graphite materials. AG, FGP and KG with low crystallinity and/or small lateral size are suitable to prepare graphenes with 1 to 3 layers.

From the above results, we suggest that the selectivity of the number of graphene layers is intrinsically attributed to the different structure of the starting graphite materials. It is well accepted that GO formation involves the reaction of graphite with strong oxidants [15–17], and the exposed carbon atoms, in particular those on the edges of the graphitic layers, are most likely to be attacked by the oxidants during the oxidation stage [25]. The starting graphite with a low crystallinity has weak interlayer interaction, easily causing the increase of *d*-spacing and configuration change from a planar sp^2-hybridized to a distorted sp^3-hybrized geometry. This increases the possibility of the diffusion of oxidants between graphitic layers. Moreover, because the diffusion route is shorter for the graphite with smaller lateral size, the oxidation and intercalation occur more easily. As a result, graphite with a small lateral size and low crystallinity can easily form well-oxidized GO under the same conditions. McAllister et al. [17] proposed that exfoliation upon rapid heating takes place only when the decomposition rate of the epoxy and hydroxyl sites of GO exceeds the diffusion rate of the evolved gases. Therefore, the exfoliation degree of TEGO derived from different starting graphites is different due to the different oxidation degree of the corresponding GO. This result can be proved by the different surface areas of TEGO derived from different starting graphites, which were 75, 50, 152, 137, and 351 m^2/g, respectively for HOPG, NFG, KG, FGP, and AG. Since the number of layers in the obtained graphene is mainly determined by the exfoliation process, we suggest that the synthesis of graphene with selected number of layers is essentially attributed to the different oxidation degrees of the starting graphites, caused by their different lateral size and crystallinity.

Normally, chemically derived graphene is electrically insulating due to the heavy oxygenation of graphene sheets, which can not be used as conductive materials and electronic devices without further processing [15]. Recent studies have demonstrated that the electrical conductivity of graphene can be dramatically improved by chemical reduction or thermal treatment [6,15,22,26]. Considering the similar atomic C/O ratio of our graphene to that of chemically reduced graphene sheets, therefore, it is reasonable to expect that the

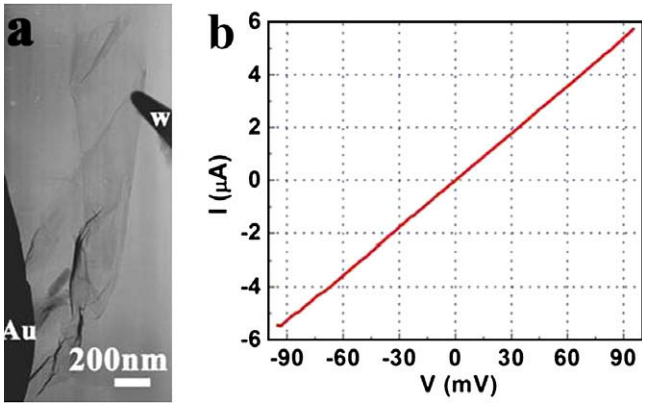

Fig. 7 – Electrical conductivity measurement of the graphene derived from AG. (a) TEM image of an individual single-layer graphene during electric conductivity measurements, using Au as electrode and tungsten as tip. (b) Typical I–V curve of the graphene in (a).

graphene obtained has an electronic transport property suitable for the application as conductive materials and electronic devices.

The electrical conductivity of individual single-layer graphene derived from AG was determined inside a HRTEM and the result is shown in Fig. 7. It is interesting to find that, similar to those prepared by micro-mechanical cleavage [2], our graphene offers a linear current-voltage (I–V) characteristic of typical metallic material in the voltage range of −90 mV–90 mV with a conductivity of $\sim 1\times10^3$ S/cm (Fig. 7b), which is ~3 orders of magnitude higher than that of individual GO reduced by hydrazine [22], and higher than that of graphene films obtained by hydrazine reduction or high temperature graphitization treatment [10,26–28]. Combining this with the above XPS results, we believe that this high conductivity is attributed to the good deoxygenation of GO to restore C–C and C=C bonds in the whole graphene layer after the reduction process [22].

4. Conclusion

A simple and effective strategy to tune the number of graphene layers by selecting suitable starting graphite is presented. Both the lateral size and crystallinity of the original graphite are found to play important roles in the number of graphene layers obtained by chemical exfoliation. The smaller the lateral size and the lower the crystallinity of the starting graphite, the fewer the number of layers in the graphene obtained. Graphite with a small lateral size and low crystallinity is appropriate to prepare single-layer graphene. Moreover, these graphenes exhibit high-quality with an electrical conductivity of $\sim 1 \times 10^3$ S/cm. These findings should enable further investigation of the physical and chemical properties of graphene with different number of layers, and open up a wide spectrum of possibilities for technological applications including nanoelectronics, sensors, composites, energy storage and absorption media, etc.

Acknowledgements

We acknowledge support by National Science Foundation of China (No.50872136 and No. 90606008), MOST of China (No. 2006CB932701), Chinese Academy of Sciences (No. KJCX2-YW-M01), and the Knowledge Innovation Program of CAS. We thank Prof. P. Thrower for kind suggestions and corrections on our paper, Dr. F. Li and Dr. O. Lourie for valuable discussion, and Mr. D. M. Tang for electric conductivity measurements.

REFERENCES

[1] Geim AK, Novoselov KS. The rise of graphene. Nature Mater 2007;6(3):183–91.
[2] Novoselov KS, Geim AK, Morozov SV, Jiang D, Zhang Y, Dubonos SV, et al. Electric field effect in atomically thin carbon films. Science 2004;306(5296):666–9.
[3] Novoselov KS, Jiang D, Schedin F, Booth TJ, Khotkevich VV, Morozov SV, et al. Two-dimensional atomic crystals. Proc Natl Acad Sci USA 2005;102(30):10451–3.
[4] Zhang YB, Tan YW, Stormer HL, Kim P. Experimental observation of the quantum Hall effect and Berry's phase in graphene. Nature 2005;438(7065):201–4.
[5] Novoselov KS, Geim AK, Morozov SV, Jiang D, Katsnelson MI, Grigorieva IV, et al. Two-dimensional gas of massless Dirac fermions in graphene. Nature 2005;438(7065):197–200.
[6] Gilje S, Han S, Wang M, Wang KL, Kaner RB. A chemical route to graphene for device applications. Nano Lett 2007;7(11):3394–8.
[7] Stankovich S, Dikin DA, Dommett GHB, Kohlhaas KM, Zimney EJ, Stach EA, et al. Graphene-based composite materials. Nature 2006;442(7100):282–6.
[8] Schedin F, Geim AK, Morozov SV, Hill EW, Blake P, Katsnelson MI, et al. Detection of individual gas molecules adsorbed on graphene. Nature Mater 2007;6(9):652–5.
[9] Liang X, Fu Z, Chou SY. Graphene transistors fabricated via transfer-printing in device active-areas on large wafer. Nano Lett 2007;7(12):3840–4.
[10] Watcharotone S, Dikin DA, Stankovich S, Piner R, Jung I, Dommett GHB, et al. Graphene-silica composite thin films as transparent conductors. Nano Lett 2007;7(7):1888–92.
[11] Wang X, Zhi LJ, Tsao N, Tomovic Z, Li JL, Mullen K. Transparent carbon films as electrodes in organic solar cells. Angew Chem Int Ed 2008;47(16):2990–2.
[12] Eda G, Fanchini G, Chhowalla M. Large-area ultrathin films of reduced graphene oxide as a transparent and flexible electronic material. Nature Nanotech 2008;3(5):270–4.
[13] Berger C, Song ZM, Li XB, Wu XS, Brown N, Naud C, et al. Electronic confinement and coherence in patterned epitaxial graphene. Science 2006;312(5777):1191–6.
[14] Niyogi S, Bekyarova E, Itkis ME, McWilliams JL, Hamon MA, Haddon RC. Solution properties of graphite and graphene. J Am Chem Soc 2006;128(24):7720–1.
[15] Stankovich S, Dikin DA, Piner RD, Kohlhaas KA, Kleinhammes A, Jia Y, et al. Synthesis of graphene-based nanosheets via chemical reduction of exfoliated graphite oxide. Carbon 2007;45(7):1558–65.
[16] Schniepp HC, Li JL, McAllister MJ, Sai H, Herrera-Alonso M, Adamson DH, et al. Functionalized single graphene sheets derived from splitting graphite oxide. J Phys Chem B 2006;110(17):8535–9.
[17] McAllister MJ, LiO JL, Adamson DH, Schniepp HC, Abdala AA, Liu J, et al. Single sheet functionalized graphene by oxidation and thermal expansion of graphite. Chem Mater 2007;19(18):4396–404.
[18] Yu AP, Ramesh P, Itkis ME, Bekyarova E, Haddon RC. Graphite nanoplatelet-epoxy composite thermal interface materials. J Phys Chem C 2007;111(21):7565–9.
[19] Li XL, Wang XR, Zhang L, Lee SW, Dai HJ. Chemically derived, ultra-smooth graphene nanoribbon semiconductors. Science 2008;319(5867):1229–32.
[20] Li D, Muller MB, Gilje S, Kaner RB, Wallace GG. Processable aqueous dispersions of graphene nanosheets. Nature Nanotech 2008;3(2):101–5.
[21] Hummers W, Offman R. Preparation of graphitic oxide. J Am Chem Soc 1958;80:1339.
[22] Gomez-Navarro C, Weitz RT, Bittner AM, Scolari M, Mews A, Burghard M, et al. Electronic transport properties of individual chemically reduced graphene oxide sheets. Nano Lett 2007;7(11):3499–503.
[23] Jung I, Pelton M, Piner R, Dikin DA, Stankovich S, Watcharotone S, et al. Simple approach for high-contrast optical imaging and characterization of graphene-based sheets. Nano Lett 2007;7(12):3569–75.
[24] Gupta A, Chen G, Joshi P, Tadigadapa S, Eklund PC. Raman scattering from high-frequency phonons in supported *n*-graphene layer films. Nano Lett 2006;6(12):2667–73.

[25] Li JL, Kudin KN, McAllister MJ, Prud'homme RK, Aksay IA, Car R. Oxygen-driven unzipping of graphitic materials. Phys Rev Lett 2006;96(17):176101.
[26] Wang X, Zhi LJ, Mullen K. Transparent, conductive graphene electrodes for dye-sensitized solar cells. Nano Lett 2008;8(1):323–7.
[27] Xu YX, Bai H, Lu GW, Li C, Shi GQ. Flexible graphene films via the filtration of water-soluble noncovalent functionalized graphene sheets. J Am Chem Soc 2008;130(18):5856–7.
[28] Becerril HA, Mao J, Liu Z, Stoltenberg RM, Bao Z, Chen Y. Evaluation of solution-processed reduced graphene oxide films as transparent conductors. Acs Nano 2008;2(3):463–70.